Title	On the type of impeller of a centrifugal blower, with special references to the problem concerning the number of impeller blades
Sub Title	
Author	渡部, 一郎(Watanabe, Ichiro)
Publisher	慶應義塾大学藤原記念工学部
Publication year	1949
Jtitle	慶應義塾大学藤原記念工学部研究報告 (Proceedings of Faculty of Engineering, Keiogijuku University). Vol.2, No.5 (1949. 7) ,p.49(5)- 71(27)
JaLC DOI	
Abstract	Experiments were performed previously by the same author on a centrifugal blower fitted with impeller, the number of blades of which being 4, 8 and 16, with the results that the larger the number of blades the better the performance characteristics. It is easily expected, however, that the further increase of the number of blades will lower the performances of the blower as the resistance of impeller channels increases. To ascertain this, experiments were performed with different centrifugal blower with impellers fitted with straight radial blades, the number of which now selected to be z=2, 4, 8, 16, 20 and 32. The optimum number of blades, in this case, is found to be z=10 ~ 12, but these figures are not applied generally to all blowers, even if the blower types were the same. In this report, the relations between the slip coefficient of impeller and the number of impeller blades are surveyed both theoretically and experimentally to find a new formula which holds quite satisfactorily with high speed blower fitted with straight radial blades.
Notes	
Genre	Departmental Bulletin Paper
URL	https://koara.lib.keio.ac.jp/xoonips/modules/xoonips/detail.php?koara_id=KO50001004-00020005-0005

On the Type of Impeller of a Centrifugal Blower, with Special References to the Problem Concerning the Number of Impeller Blades.

Recieved April, 12, 1949. Ichirō Watanabe*

Experiments were performed previously by the same author on a centrifugal blower fitted with impeller, the number of blades of which being 4, 8 and 16, with the results that the larger the number of blades the better the performance characteristics. It is easily expected, however, that the further increase of the number of blades will lower the performances of the blower as the resistance of impeller channels increases. To ascertain this, experiments were performed with different centrifugal blower with impellers fitted with straight radial blades, the number of which now selected to be $z=2, 4, 8, 16, 20$ and 32. The optimum number of blades, in this case, is found to be $z=10\sim12$, but these figures are not applied generally to all blowers, even if the blower types were the same. In this report, the relations between the slip coefficient of impeller and the number of impeller blades are surveyed both theoretically and experimentally to find a new formula which holds quite satisfactorily with high speed blower fitted with straight radial blades.

I. Introduction

Experiments were performed previously on a centrifugal blower fitted with impeller, the number of blades z of which being 4, 8 and 16, to find the optimum number of impeller blades, i.e. the number which gives the best performances[1]. According to the results of these experiments, the optimum number of impeller blades was found to be $z=16$.

It is easily expected, however, that the further increase of the number of blades will lower the performances of the blower as the resistance of impeller channels increases, but these points were remained unsolved. To ascertain this, experiments were performed with different centrifugal blower with impellers fitted with straight radial blades, the number of which now selected to be $z=2, 4, 8, 16, 20$ and 32.

Various experiments were hitherto performed concerning the number of impeller

* Dr. of Eng., Prof. of Keiogijuku University.

1) Ichirō Watanabe; Rep. of the Inst. of Aeronautics **159** (1937).

blades[2,3]. Further, theoretical surveys upon this item were performed by W. Kucharski[4], E. Sörensen[5], W. Scutz[6] and A. Busemann[7]. Especially as to the slip coefficients of impeller with various number of blades were investigated by B. Eck[8], Stodola[9] and Pfleiderer[10]. T. Baumeister staies in his text[11] that the optimum number of impeller blades of a centrifugal blower is not constant but affected by the type of the blower. Also, it is considered to vary by the diameter ratio of the impeller, i.e. the diameter ratio of the exit and the inlet diameter, should the type of the blower be the same. It is necessary, therefore, to bring to light this problem, treating the item theoretically with aids of a large number of experiments. In this report, the optimum number of blades is found to be $z=10\sim12$ for high speed blower fitted with straight radial blades, but these figures are not applied generally to all blowers even if the blower types were the same. The general tendency, as T. Baumeister said, is that the optimum number decreases as the increase of diameter ratio, i.e. as the increase of blade length. This tendency seems to hold so far as the experiments carried by the author, but it is necessary to collect further experimental results to formulate this effect.

In this report, however, the relations between the slip coefficient of impeller and the number of impeller blades are surveyed both theoretically and experimentally to establish a new formula which holds quite satisfactorily with high speed blower fitted with straight radial blades, leaving the diameter ratio effect unsolved.

II. Experimental Installation and Impellers used.

The centrifugal blower used in the present experiments is fitted with impeller of straight radial blades, and is driven by an electric dynamometer of 20 HP. The mass flow of air was measured by an orifice fitted in the suction pipe of the blower, and experiments were performed by delivery throttling. Measurements were made as to the suction pressure p_s, suction temperature t_s, delivery pressure p_d, delivery temperature t_d. Further, the pressure and temperature distributions within the impeller and diffuser were measured by mercury manometers and thermocouples respectively, the number of measuring points were 4 in the impeller and 3 in the

2) W. J. Kearton, Proc. Inst. Mech. Engineers, **124** (April 1933) 481—568.
3) Fechheimer, Trans. A.S.M.E., **46** (1924) 287—347.
4) W. Kucharski, Strömung einer reibungsfreien Flüssigkeit bei Rotation fester Körper (1918).
5) E. Sörensen, Z.A.M.M. (April 1927) 89.
6) W. Schulz, Forschungsarbeiton, **307** (1928).
7) A. Busemann, Z.A.M.M. (October 1928) 372.
8) B. Eck, Ventilatoren (1937) 29—30.
9) Stodola, Dampf- und Gasturbinen, (1924) 1045—1049.
10) Pfleiderer, Die Kreiselpumpen.
11) T. Baumeister, Fans (1935).

diffuser. The hot junction of the thermocouple used is fitted within the hole of a small screw of bakelite, and this small screw were set into the casing wall, thus preventing the temperature of casing to disturb the readings.

The impeller shaft of this blower is driven by an electric dynamometer through a step-up gear, the gear ratio of which being 6.818. The diffuser used is fitted with no guide vanes. Impellers have, as seen in fig. 1, straight radial blades, the outside diameter being 240 mm, the number of blades z being selected as $z=2, 4, 8, 16, 20$ and 32. Fig. 2 shows the positions at which the pressures and temperatures of impeller or diffusser are measured.

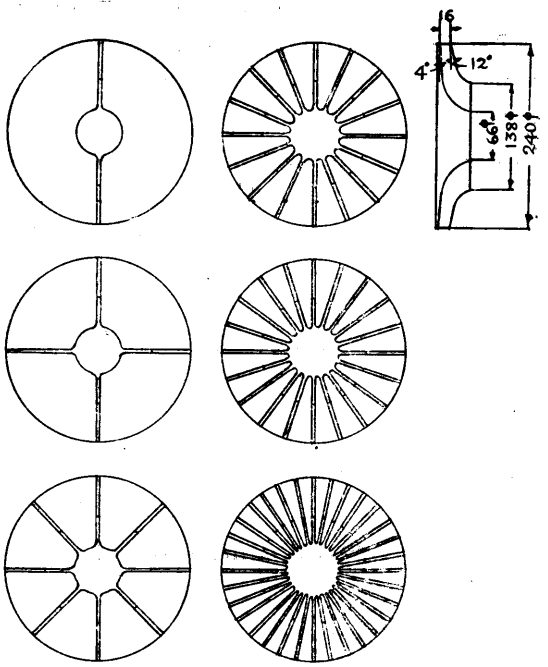

Fig. 1. Impeller used with Straight radial blades.

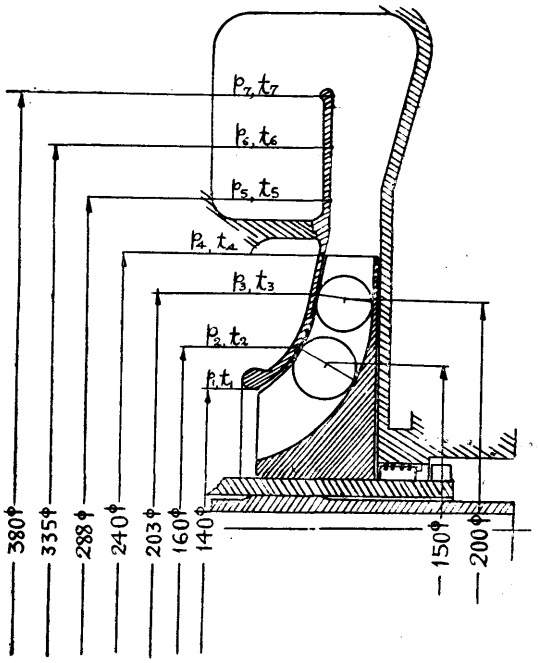

Fig. 2. Positions for measurement of pressure and temperature distributions within impeller channel and diffuser.

III. Experimental results.

3.1 Comparison of overall performances.

The results of experiments are corrected by means of dimensional analysis[12]. The overall adiabatic efficiency of the blower is calculated by the expression

$$\eta_0=\left[\frac{k}{k-1}\frac{RGT_s}{75}\left\{\left(\frac{p_d}{p_s}\right)^{\frac{k-1}{k}}-1\right\}+\frac{G}{2g\times 75}(w_d^2-w_s^2)\right]\Big/P$$

where P: driving HP of the blower, G: mass flow of air kg/sec, w_d: air velocity in the delivery pipe, m/sec, w_s: air velocity in the suction pipe m/sec, p_d: delivery pressure, p_s: suction pressure, T_s: suction temperature ^0K. The adiabatic temp-

12) R. S. Capon, G. V. Brooke, R. & M. 1336.

erature efficiency η_t is calculated by the expression

$$\eta_t=(T-T_s)/(T_d-T_s),\quad T=T_s(p_d/p_s)^{\frac{k-1}{k}}$$

The relations between pressure ratio p_d/p_s and volume flow of air V_s at the suction inlet at the impeller rotations n=15000 r.p.m., impeller tip speed u=188.5 m/sec are shown in fig. 3. Although the pressure ratios when the number of blades z are small, i.e. 2 and 4 show relatively lower values, they attain nearly constant values

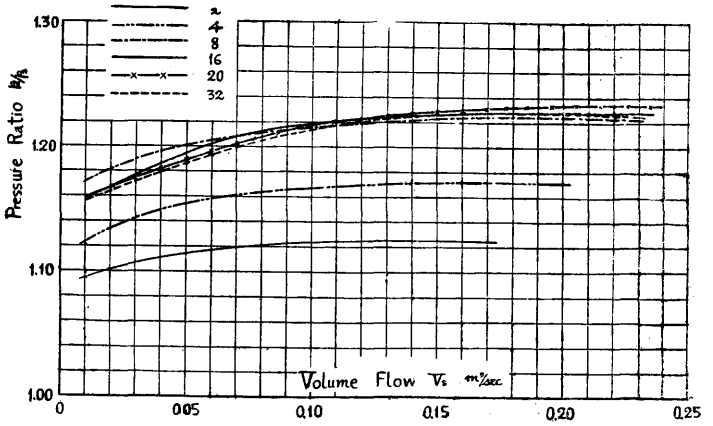

Fig. 3. Relations between pressure ratio p_d/p_s and V_s
[n=15000 r.p.m., u=188.5 m/sec]

when z exceeds 8, the pressure ratios increasing as z increases till z=20, but falls slightly when z attains 32. Fig. 4 shows the relations between the temperature ratio T_d/T_s and volume flow of air V_s when u=188.5 m/sec. The relations between driving HP and volume flow V_s at the same peripheral speed of the impeller are shown

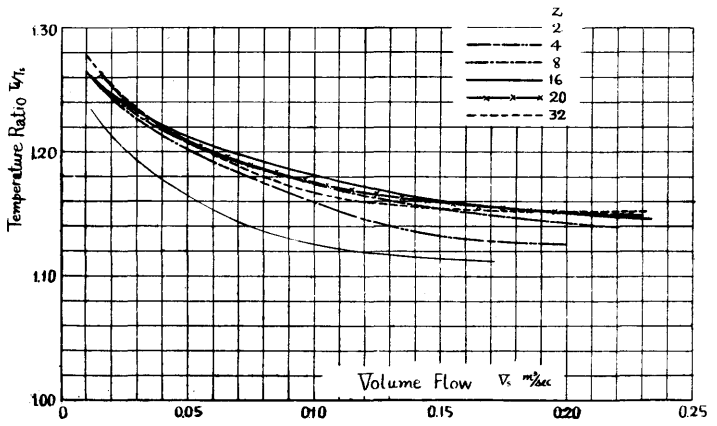

Fig. 4. Relations between temperature ratio T_d/T_s and V_s.
[n=15000 r.p.m., u=188.5 m/sec]

in fig. 5, to find the driving HP increasing as the number of blades. The relations

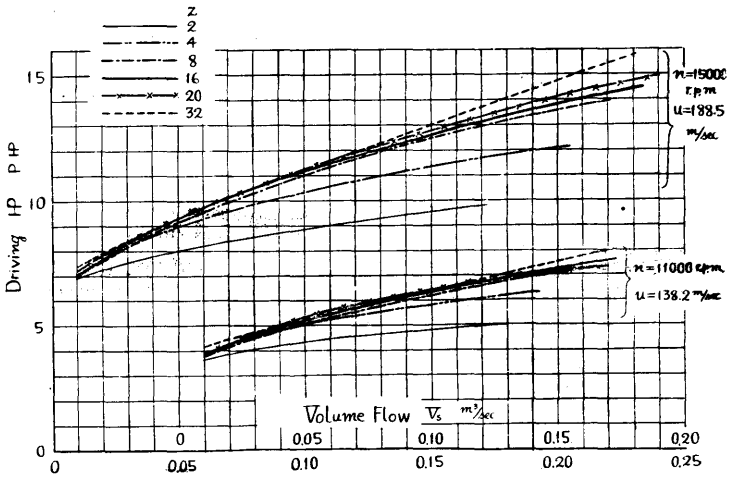

Fig. 5. Relations between driving HP P and V_s.

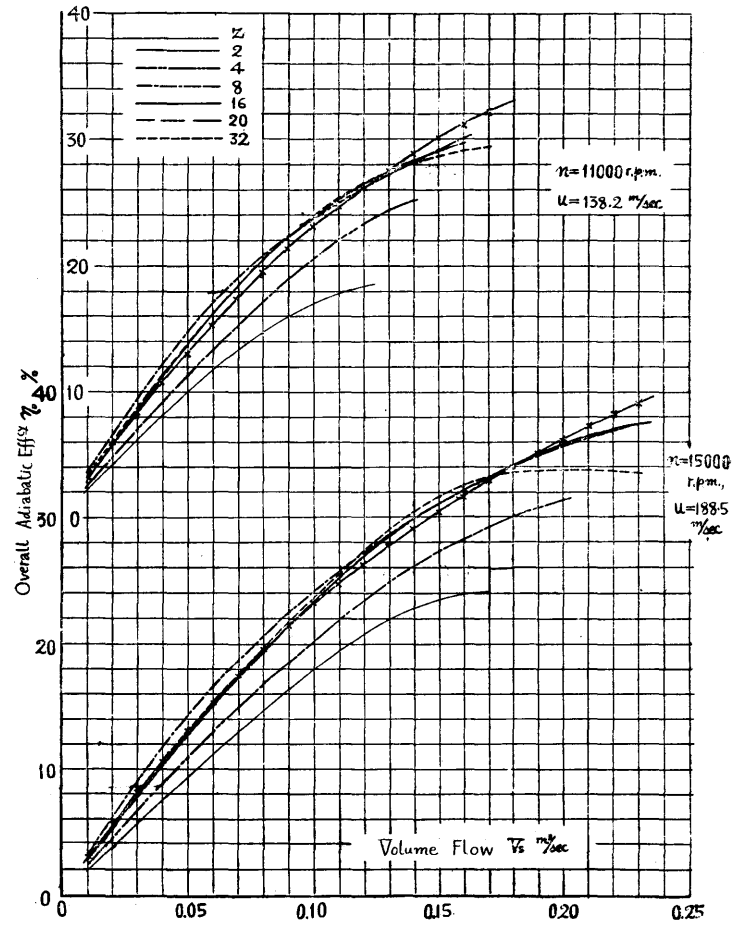

Fig. 6. Relations between overall adiabatic efficiency η_0 and V_s.

between overall adiabatic efficiency η_0 and V_s are shown in fig. 6, while that between adiabatic temperature efficiency η_t and V_s are shown in fig. 7.

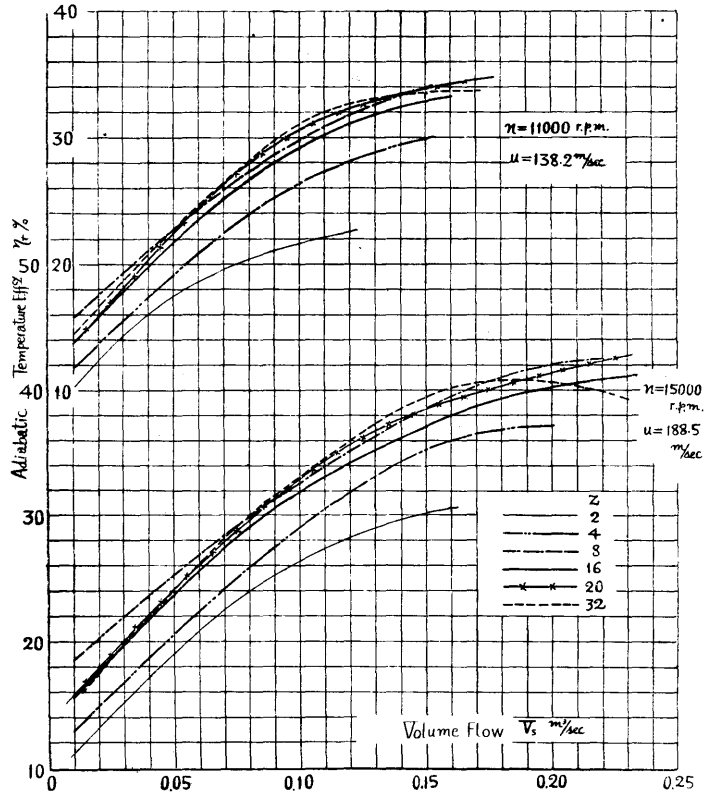

Fig. 7. Relations between adiabatic temperature efficiency η_t and V_s.

In order to realize the above-mentioned results more completely, pressure ratio p_d/p_s is plotted against the number of impeller blades z taking V_s as parameter, when peripheral velocity of impeller u=188.5 m/sec, as shown in Fig. 8. As is seen from the figure, pressure ratios are maximum in the range of z= 10~12, while pressure ratios becoming smaller gradually when z exceeds the foregoing values. Fig. 9 shows the temperature ratio T_d/T_s which represents nearly the same tendency

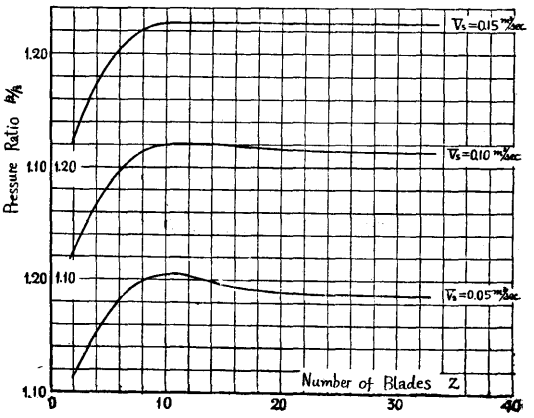

Fig. 8. Relations between pressure ratio p_d/p_s and number of blades [n=15000 r.p.m., u=188.5 m/sec].

as pressure ratio. The relations between the driving HP and z are plotted in fig. 10, in which P remains nearly constant when z exceeds $z=10$. The overall adiabatic efficiency η_0 reaches its maximum value when z attains 10 or so (Fig. 11). Fig. 12 is the relations between adiabatic temperature efficiency η_t and z, which shows the same tendency as η_0.

Now, it is seen from the above-mentioned general performance characteristics of the blower that the performance is optimum at $z=10\sim12$. The experiments carried on formerly on a centrifugal blower with straight radial blades impeller showed the results that the performance is optimum at the range of impeller blades of z of 16 or more. In that case, the outside diameter D_2 and inlet diameter D_1 of the impeller are $D_2=206$ mm and $D_1=135$ mm, with the result that the diameter ratio $D_2/D_1=1.526$, while in this case, the impeller dimensions are $D_2=240$ mm, $D_1=138$ mm and $D_2/D_1=1.740$. As stated in the introduction of this report, the number of blades at which the blower shows optimum performance decreases as the blade length increases, i.e. the diameter ratio D_2/D_1 increases. The fact is suggested by T. Baumeister and is generally accepted. This fact holds also in our cases. The optimum number of blades $z=10\sim12$ in this case, however, does not hold in the other cases

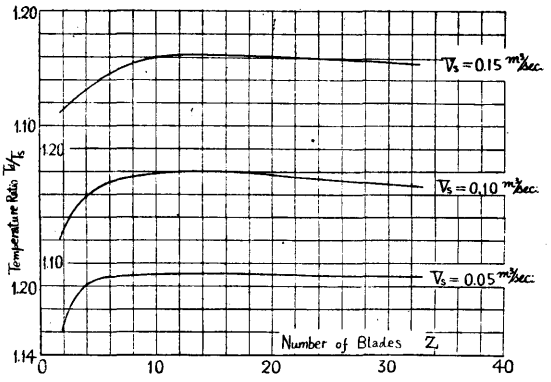

Fig. 9. Relations between temperature ratio T_d/T_s and z [$n=15000$ r.p.m., $u=188.5$ m/sec].

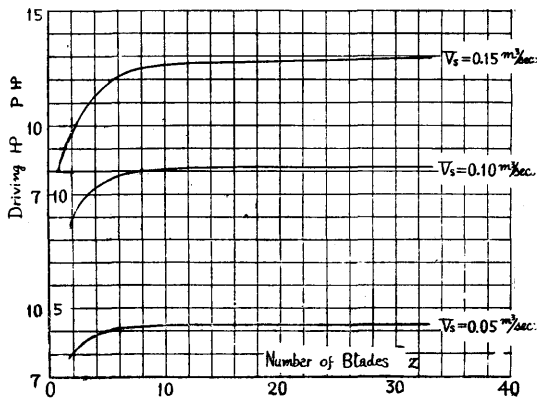

Fig. 10. Relations between driving HP P and z [$n=15000$ r.p.m., $u=188.5$ m/sec].

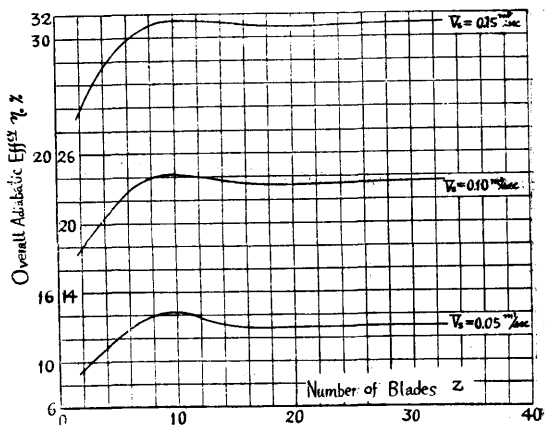

Fig. 11. Relations between overall adiabatic efficiency and z [$n=15000$ r.p.m., $u=188.5$m/sec]

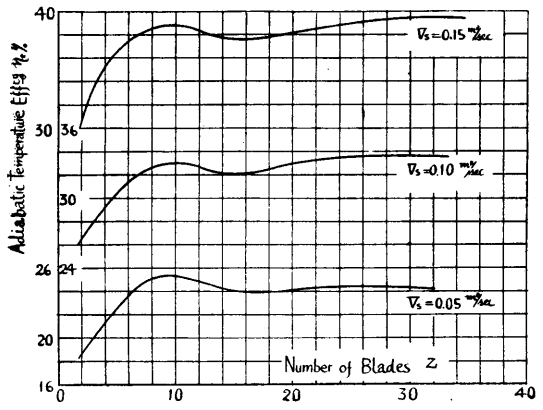

Fig. 12. Relations between adiabatic temperature efficiency η_t and z [$n=15000$ r.p.m., $u=188.5$ m/sec].

even if the impeller type be the same. The factors which gives large influence to the optimum number seems to be the diameter ratio of the impeller, but it is unable to clearify this effect in this case for the lack of experimental results.

3.2 Slip coefficient of impeller.

Pressure distributions and temperature distributions at the impeller channel and the diffuser were corrected to standard suction pressure and temperature by dimensional relationships of the blower, and from these corrected values it is able to evaluate the slip coefficient of impeller. The formula which gives the slip coefficient of the straight radial blades impeller such as used in these experiments is

$$K\frac{u_4^2}{g}=\frac{1}{2g}(w_4^2-w_s^2)+\frac{k}{k-1}RT_s\left\{\left(\frac{p_4}{p_s}\right)^{\frac{k-1}{k}}-1\right\}$$

where u_4: peripheral velocity at the exit of the impeller, w_s: absolute velocity of air just before the impeller inlet, w_4: that at the impeller exit, p_4: static pressure at exit of the impeller channel, p_s: static suction pressure[13], T_s: suction temperature absolute[13].

p_4, p_s and T_s are known from experimental data, while w_s and w_4 are calculable by means of the relations $w_s=GRT_s/A_sp_s$, $w_4^2=u_4^2+w_{14}^2$, $w_{14}=GRT_4/A_4p_4$ and $A_4=2\pi r_4b_4-zt_4$, where p_4, T_4: pressure[14] and absolute temperature at the exit of the impeller channel respectively, A_4: exit area of the impeller channel perpendicular to the direction of flow, b_4: width of blade at the impeller exit, the radius of which being r_4, t_4: thickness of blade at the impeller exit, z: numbers of impeller blades. Therefore, it is able to calculate the slip coefficient of impeller K from the foregoing expression.

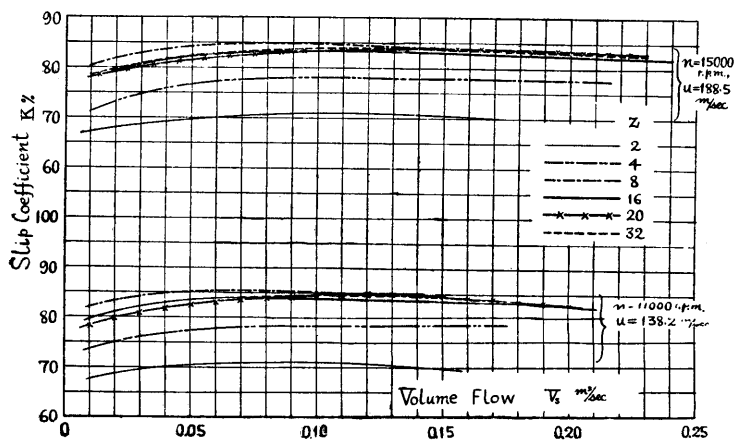

Fig. 13.
Relations between slip coefficient K and z_s.

13) p_s and T_s are considered here as the pressures and temperatures just before the impeller inlet.

14) Hereafter static pressures are represented merely as pressures.

Fig. 13 shows the relations between the slip coefficient of impeller K thus obtained and the volume flow of air V_s for the case of u=188.5 m/sec and u=138.2 m/sec. The forms of the curves resemble that of the pressure. These relations are replotted against the number of blades z for the case of u=188.5 m/sec, as in fig. 14, to find the maximum value of K=9~11, while decreasing slightly as z increases further.

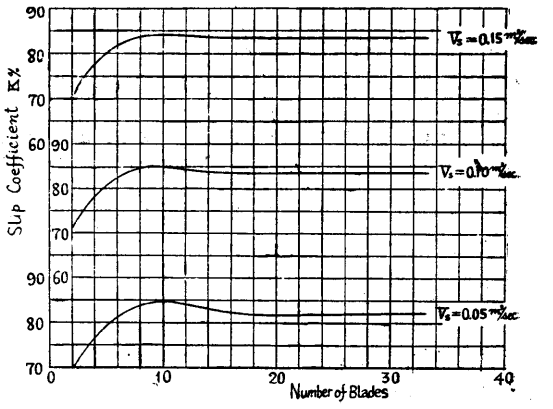

Fig. 14. Relations between slip coefficient K and number of blades [n=15000 r.p.m., u=188.5 m/sec].

3.3 Relations between the absolute velocity of air and the pressure in the impeller channel.

In the impeller channel, air particles are given centrifugal forces, thus increasing both the absolute velocity and the pressure. To investigate the impeller works in good condition or not, it is therefore necessary to consider the relations between the absolute velocity of air $w=\sqrt{u^2+w_r^2}$ [15] at arbitrary point in the impeller channel and the pressure at the same point, where u means the peripheral velocity at the point now considered, w_r means the relative velocity of air at the same point. Assuming air flows uniformly in the impeller channel, it is able to calculate the relative velocity of air w_r at the points where pressure and temperature distributions were measured. Using this ualue of w_r, w is enumerated from the above expression, and the relation between the w^2 and pressure in the case of u=188.5 m/sec

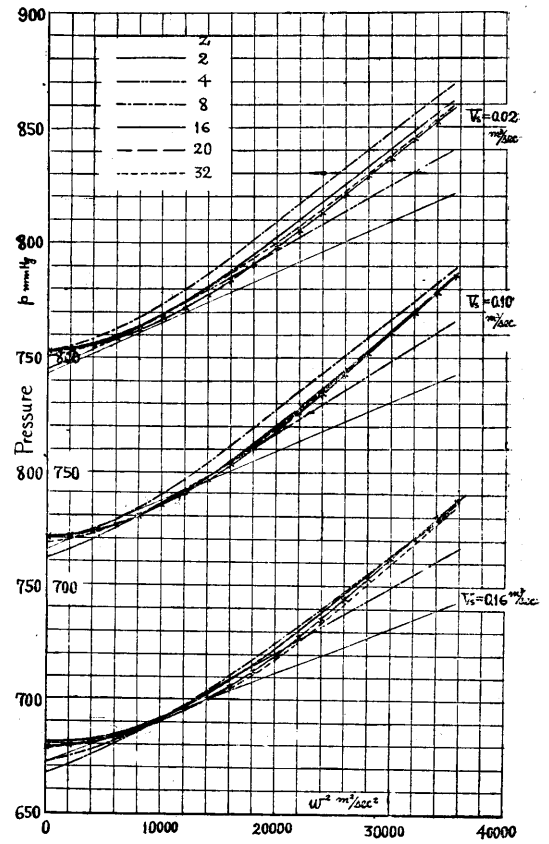

Fig. 15. Relations between pressure p and w^2 [n=15000 r.p.m., u=188.5 m/sec].

15) This relation holds because of the straight radial blades.

are shown in fig. 15. We are able to judge the working condition of the impeller channel to be better as the pressure is higher for the same value of w^2. It is plain from the figure that the case of $z=8$ is most favourable, while the working condition of the impeller channel becoming less effective in the case of $z=16$, 20 and 32.

IV. Considerations on the slip coefficient of impeller.

As stated already in the introduction, the slip coefficient as functions of the number of impeller blades was studied by B. Eck, Stodola and Pfleiderer. Particularly, B. Eck gave in his text book[16] the method of obtaining the slip coefficient graphically from the pressure differences between the positive pressure side and negative pressure side of the blades using the calculated Values of the relative velocities in the impeller channel. The evaluated values of the slip coefficient for the case of backward curved blade impeller, radial exit blade impeller and forward curved blade impeller are shown in the same literature. It is considered worthwhile, therefore, to check whether the calculated values of the slip coefficient K by this B. Eck's graphical method to coincide or not the experimentally obtained values of K in the present case. Unfortunately, the values of K obtained by B. Ecks method deviate from the values of K obtained experimentally so far as the straight radial blades impeller is concerned. We are able to find, however, that the calculated results to coincide fairly well with the experimental one with the aids of proper assumptions obtained from the photographic study[17] of the flow patterns of the air flow within the impeller channel by "Schlieren" method.

The graphical method of calculation of K is, however, tedious and is considered unsuitable for practical use. The author, therefore, introduced the formula of the slip coefficient K of impeller as functions of number of blades z from the considerations of the relative velocity distributions within the impeller channel. The values obtained by this formula does not perfectly coincide with the experimental one, but it gives the closer value than that of formulas of B. Eck and Stodola so far as the straight radial blades are concerned. The formulas given by Eck and Stodola coincide closely with the experimental values obtained by Kearton[18] on backward curved blades impeller, but they deviate not only numerically but also qualitatively with the experimental one of the straight radial blades impeller, to find them not applicable in the latter cases.

4.1 Considerations on the graphical calculus of the slip coefficient.

As impellers used in these experiments are of types shown in fig. 1, it is able to calculate the distributions of relative velocities w_r in the impeller channel from the observed values of pressure and temperature distributions by means of calculation

16) B. Eck, Ventilatoren (1937) 29—30.

17) I. Watanabe, G. Onoue, Rep. of the Inst. of Aero. **286** (March 1944).

18) Same as quoted in 8).

method already published[19]. In this case, we must use the following values, namely $\alpha=12-4=8°$, $r_2=0.120$ m, $r_0=\frac{0.069+0.033}{2}=0.051$ m, $b_2=0.016$ m, $\omega=1571$/sec ($n=$ 15000 r.p.m.). The results thus obtained are shown in fig. 16 and fig. 17 for the case

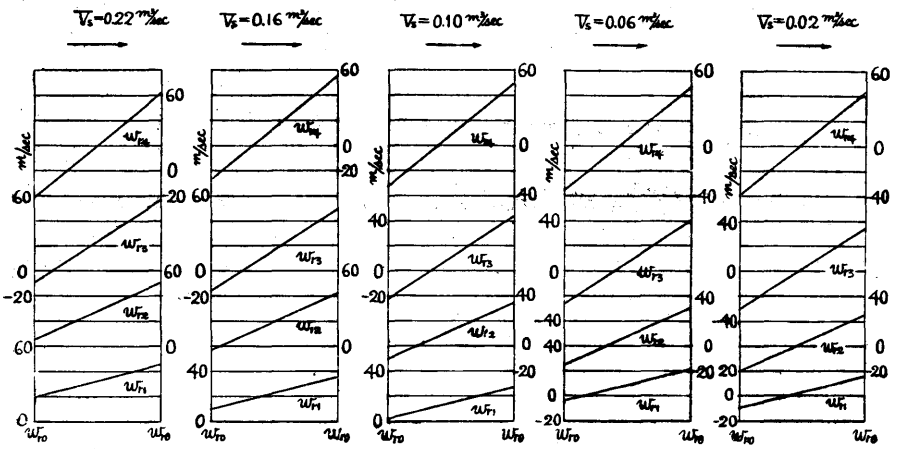

Fig. 16. Relative velocity distributions [$z=32$, $n=15000$ r.p.m.]

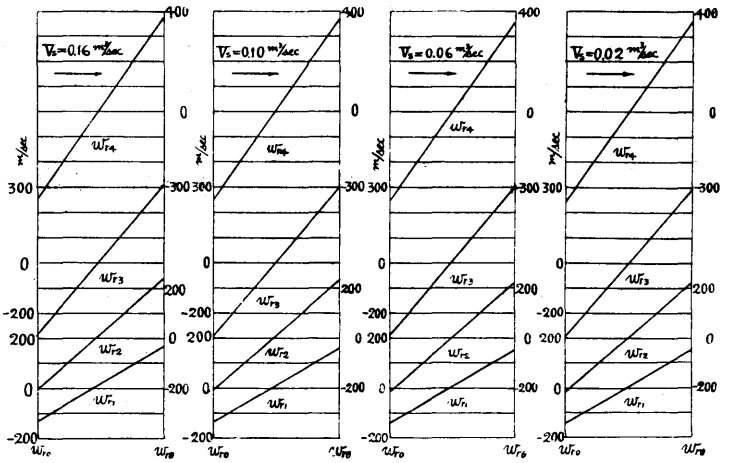

Fig. 17. Relative velocity distributions [$z=4$, $n=15000$ r.p.m.]

of $z=32$ and $z=4$ respectively. These are the cases of impeller revolutions per minute $n=15000$ r.p.m., peripheral velocity of impeller at the tip $u=188.5$ m/sec, and the velocity distributions are shown for the case of $V_s=0.22$, 0.16, 0.10, 0.06 and 0.02 m³/sec. Further, in a specified impeller channel shown, the left hand side is the positive pressure side of the blade, while right hand side indicates the negative pressure side of the blade. w_{r1}, w_{r2}, w_{r3} and w_{r4} in the figures are, of course, the calculated values of relative velocities at points where pressure and temperature distributions

19) loc. cit. in 18). The impellers in this case correspond to the type II in this literature.

are measured. It seems from the figures that the enumerated relative velocities are influenced too severely by the impeller revolutions. In other words, even as for the case of maximum volume flow, the values of w_{r3} and w_{r4} at the pressure side of blade are still negative. This seems to suggest that the expression used in the calculus involves the terms which affected by impeller revolutions too intensively. Further, as is clear in fig. 17, i.e. when $z=4$, the values of the relative velocities w_r exceeds that of sound, which is considered to be unreasonable. These facts indicate, therefore, that the application of the expression for the calculus of the relative velocities to such a high speed impeller as this case is somewhat unnatural.

Hence, the author intended to modify the hitherto used expression to be applicable to such a high speed impeller as this case. In the introduction of the expression for the caluculus of relative velocities, it has be assumed that the air flows fully in the impeller channel in radial direction, i.e. the slip coefficient K in the following expresstion

$$K\frac{1}{g}(\sigma_2 u_2-\sigma_1 u_1)=\frac{1}{2g}(w_2^2-w_1^2)+\int_{p_1}^{p_2} vdp \qquad \cdots(1)$$

is taken as $K=1$. But, as is plain from the photographic flow patterns[20] of the relative flow in the impeller channel of fig. 18, air flows mainly in the region near the negative pressure side of blade, while that near the positive pressure side no flow patterns are observed. From this fact, it is unreasonable to assume $K=1$ in the expression (1). Leaving K in expression (1) and assuming (1) to hold on every point in impeller channel, we have as previously

$$\int_{p_1}^{p} vdp=\frac{1}{2g}(u^2-u_1^2)+\frac{1}{2g}(w_{r1}^2-w_r^2)+\frac{1}{2g}(w^2-w_1^2)(K-1)$$

If the compression be adiabatic, using the relation of

$$\int_{p_1}^{p} vdp=\frac{k}{k-1}(pv-p_1v_1)$$

we have

$$\frac{k}{k-1}(pv-p_1v_1)=\frac{1}{2g}\{(u^2-u_1^2)-(w_r^2-w_{r1}^2)-(w^2-w_1^2)(1-K)\}$$

In the case of straight radial blades impeller, there holds the relation $w^2=w_r^2+u^2$. Therefore,

$$\frac{k}{k-1}(pv-p_1v_1)=\frac{1}{2g}\{K(u^2-u_1^2)-(2-K)(w_r^2-w_{r1}^2)\} \qquad \cdots(2)$$

On differentiating partially the above equation by θ, we obtain the following equation[21].

$$\frac{\partial p}{\partial\theta}=-\frac{p}{RTg}(2-K)w_r\frac{\partial w_r}{\partial\theta} \qquad \cdots(3)$$

20) Flow patterns in other cases are shown in reference 18).

21) The equation hitherto used is the form of $\frac{\partial p}{\partial\theta}=-\frac{p}{RTg}w_r\frac{\partial w_r}{\partial\theta}$, which of course coincides with (3) when $K=1$.

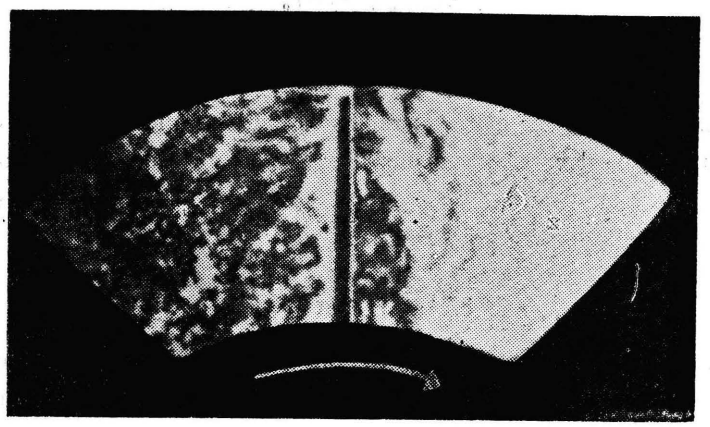

Fig. 18 (a). $z=4$, $n=7000$ r.p.m.
$\phi=10\%$, $G=0.0010$ kg/sec.

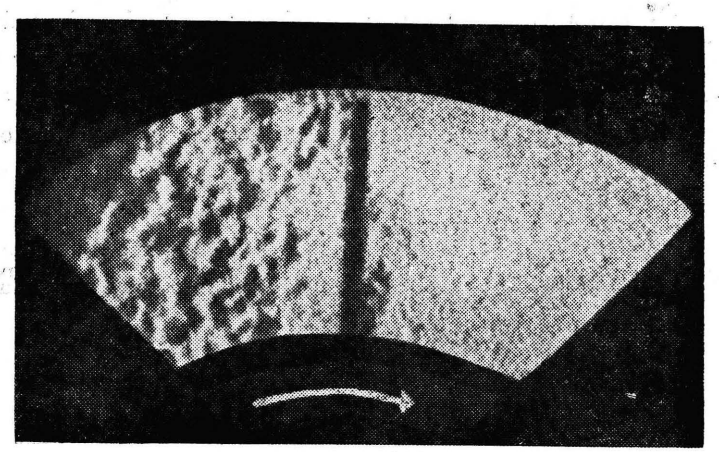

Fig. 18 (b). $z=8$, $n=7000$ r.p.m.
$\phi=100\%$, $G=0.00625$ kg/sec.

On the other hand, the equation established by the assumption that the air flows radially, i.e. the mass acceleration forces and the pressures working on the small element in the impeller channel be in equilibrium, is same as previous method[22], the result of which is as follows.

$$-\frac{\partial p}{\partial \theta}\left(1+\frac{db}{2}\right)=-2\omega w_r \frac{p}{RTg} r(1+db) \qquad \cdots (4)$$

From (3) and (4), we have

$$\frac{\partial w_r}{\partial \theta}\frac{1+\frac{db}{2}}{1+db}-2\omega r\frac{1}{2-K}=0 \qquad \cdots (5)$$

Solving equation (5), using the relation

22) The deduction of this equation is published in 18).

$$\frac{1+\frac{db}{2}}{1+db}=\frac{1+\frac{r_2-r_0}{2b_2}\tan\alpha}{1+\frac{r_2-r_0}{b_2}\tan\alpha}$$

where r_2: radius of impeller exit, r_0: radius of impeller inlet, b_2: width of blade at impeller exit, ω: angular velocity of impeller, we obtain the following solution.

$$w_r=\frac{2\omega r}{\dfrac{1+\frac{r_2-r_0}{2b_2}\tan\alpha}{1+\frac{r_2-r_0}{b_2}\tan\alpha}}\theta\frac{1}{2-K}+C \qquad \cdots(6)$$

To make the value of K not equal to unity means, as already mentioned, that the flow within the impeller channel to be partial flow. As is shown in fig. 19 (a), if we represent the angle at which the relative velocity w_r reaches the value of zero by θ_0, we are able to consider that in the domain covering the angle θ_0 there takes place no flow or reverse flow of air, as is clear from fig. 18, in other words, this domain to be the so-called dead water region. We, therefore, assume, that this region $w_r=0$. In these understandings, we put $w_r=0$ when $\theta=\theta_0$ in equation (6), to find

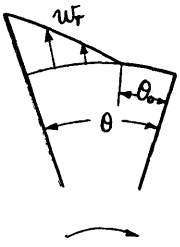

Fig. 19 (a).

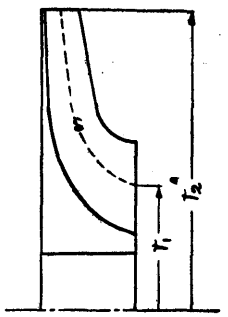

Fig. 19 (b).

$$C=-\frac{2\omega r}{\dfrac{1+\frac{r_2-r_0}{2b_2}\tan\alpha}{1+\frac{r_2-r_0}{b_2}\tan\alpha}}\theta_0\frac{1}{2-K}$$

and equation (6) becomes

$$w_r=\frac{2\omega r}{\dfrac{1+\frac{r_2-r_0}{2b_2}\tan\alpha}{1+\frac{r_2-r_0}{b_2}\tan\alpha}}\frac{1}{2-K}(\theta-\theta_0) \qquad \cdots(7)$$

The volume flow of air is calculated, therefore, as the integral of w_r between the angles of θ and θ_0, thus

$$\frac{V}{zbr}=\int_{\theta_0}^{\theta}w_r d\theta=\frac{\omega r}{\dfrac{1+\frac{r_2-r_0}{2b_2}\tan\alpha}{1+\frac{r_2-r_0}{b_2}\tan\alpha}}\frac{1}{2-K}(\theta-\theta_0)^2 \qquad \cdots(8)$$

Hence, we can obtain θ_0 which is unknown from the equation (8) if we acquainted with V, and using this value of θ_0 we can obtain w_r by equation (7).

If we represent the relative velocity w_r at the blade surface of negative pressure side by $w_{r\theta}$, we can easily see that the pressure difference between the both sides of blade $\Delta h=w_{r\theta}^2/2g$ on account of the fact that the relative velocity at the blade surface of positive pressure side w_{r_θ} is zero. Therefore, the force which acts on unit length of blade surface, the breadth of which being b, is found to be

$$P=\Delta h\cdot b\cdot\gamma \qquad \cdots(9)$$

where γ denotes the density of air at the region considered.

The turning moment at the radius r for the total blades, is,

$$M_t=zPr=z\cdot\Delta h\cdot b\cdot\gamma\cdot r \qquad \cdots(10)$$

Integrating M_t in equation (10) from r_1 to r_2 along the path s in fig. 19 (b), we have

$$M=\gamma z\int_{r_1}^{r_2}\Delta h\,br\,ds \qquad (11)$$

Denoting the theoretical work done of adiabatic compression by H, volume flow of air at suetion pipe by V_s and air density at suction pipe by γ_s, we have at once

$$M=\frac{1}{\omega}\gamma_s V_s H \qquad (12)$$

Hence, if we know M from equation (11), we are able to find H by means of equation (12), and further, we can obtain the slip coefficient of impeller K by the following relation:

$$K\frac{u^2}{g}=H \qquad \cdots(13)$$

We thus able to obtain the value of K graphically by the foregoing course. But we know that equations (7) and (8) already involve K which is not yet known. Therefore, we must proceed by cut and try method, that is, assigning K some value and putting this value into the equations (9) and (10) and further integrating graphically along the path s in fig. 19 (b) we obtain M, thus finding K by equations (12) and (13) successively. The value of K thus obtained is not always coincide the assumed value of K in equations (7) and (8). And so, we must repeat the process several times until the assumed value of K coincide that of obtained by (13). In these calculations, we take $\Delta h=0$ at the blade inlet of radius r_1, because as is clear from fig. 19 (b) the relative velocities on both sides of blade at this point must be equal.

The values of K thus obtained coincide the experimental results fairly well at the region of z which exceeds 8, while in the region $z<8$ it deviates. Now, observing again the photographic flow patterns in fig. 18, we find that there appears some small flow at the positive pressure side of blade when $z<8$[23]. Let us put the relative velocity of this small flow to be $w_{r\theta}=xw_{r\theta}$, where $w_{r\theta}$ is the relative velocity at the

23) To know more precisely, the readers should refer to the literature 17).

negative pressure side of blade. Taking account of this relative velocities of small flow, the pressure at the positive pressure surface of blade must decrease. Hence we have

$$\Delta h=\frac{1}{2g}(w_{r\theta}^2-w_{r_0}^2)=\frac{w_{r\theta}^2}{2g}(1-x^2) \qquad \cdots(14)$$

instead of $\Delta h=w_{r\theta}^2/2g$.

We have no means of evaluating the magnitudes of the relative velocity w_{r_0} of this small flow, but we are aquainted from photographic observations that the small flow increases as the number of blades z decreases. The author, therefore, proceed to select the value x such that the results obtained coincide with experimental one. The results of calculation, using the values of $x=0.27$ for $z=2$, $x=0.16$ for $z=4$, $x=0$ for $z>8$ are shown in fig. 20, to find the enumerated values coincide with experimental one. Thus the graphical calculation method of the slip coefficient of impeller hitherto used by B. Eck and others cannot be applied directly to the high speed impeller of straight radial blades. But, addition of the two assumptions based on the observation of the photographic study of the relative flow, i.e. the assumption of partial flow and generation of small flow at the blade surface of positive pressure side brings the graphical enumeration method to be applicable in the high speed impeller. B. Eck performed the evaluation of the slip coefficient K for the case of backward curved blades impeller, radial exit blades impeller and forward curved blades impeller taking with an example, and gave the values of K to be 0.862, 0.866 and 0.778 respectively when the blade width converges towards the tip. But he did not compare his results with experiments. Therefore, it seems doubtful whether the results thus obtained coincide with experimental results as to the number of blades.

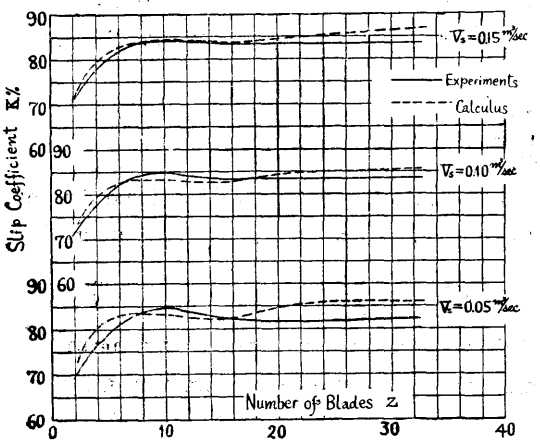

Fig. 20. Comparison of experimental results with graphical calculation for slip coefficient of impeller [u=15000 r.p.m., n=188.5 m/sec].

With the values of K obtained for various number of blades, it is able to calculate the relative velocity distribution within the impeller blades using again the equations (7) and (8). These results for $z=32$, 20, 16, 8, 4 and 2 are plotted in fig. 21~fig. 26. In these cases, the values of w_r does not exceed the velocity of sound even when the number of blades be small, that is, when $z=4$ and 2, and from this we can recommend equations (7) and (8) to be applicable for high speed impeller of straight radial blades.

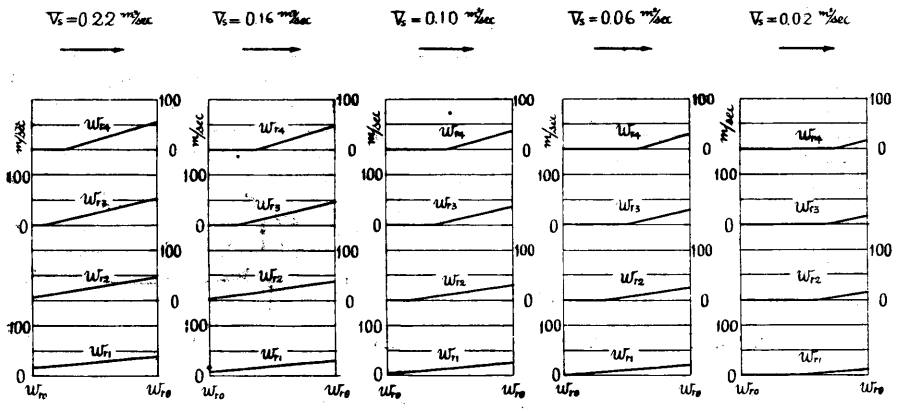

Fig. 21. Relative velocity distributions [$z=32$, $n=15000$ r.p.m.].

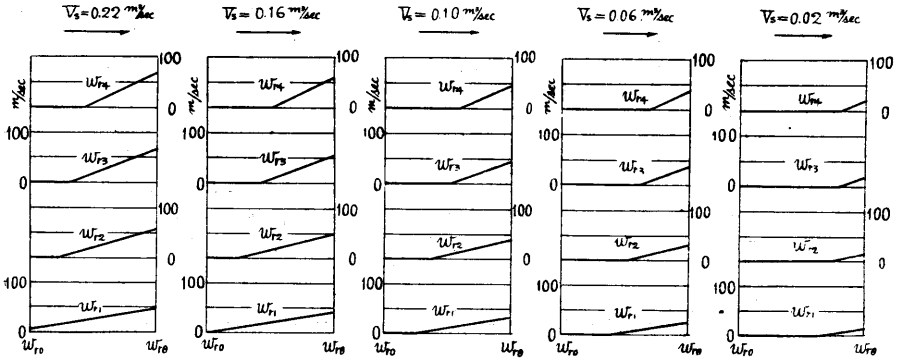

Fig. 22. Relative velocity distributions [$z=20$, $n=15000$ r.p.m.].

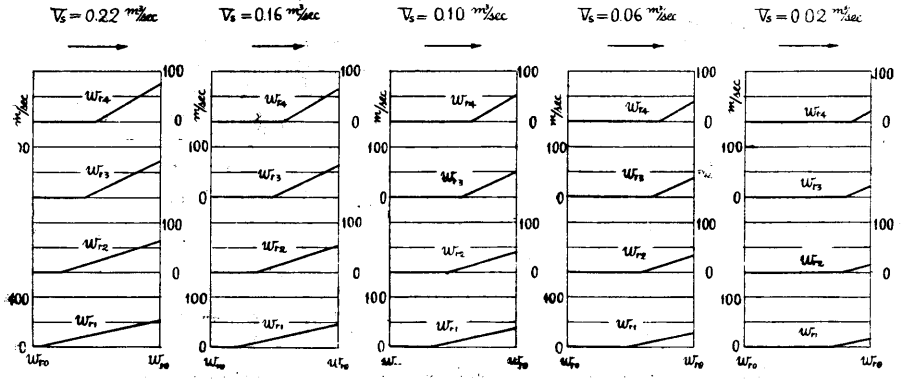

Fig. 23. Relative velocity distributions [$z=16$, $n=15000$ r.p.m.].

Plotting the delivery pressure p_d against the suction volume flow V_s for the cases of various number of blades and extending the curves towards the region of large values of V_s, we are able to find the values of volume flow $V_{s\,p_d=0}$ that is the volume flow when $p_d=760$ mm Hg or pressure rise $\Delta p_d=0$. These values for the

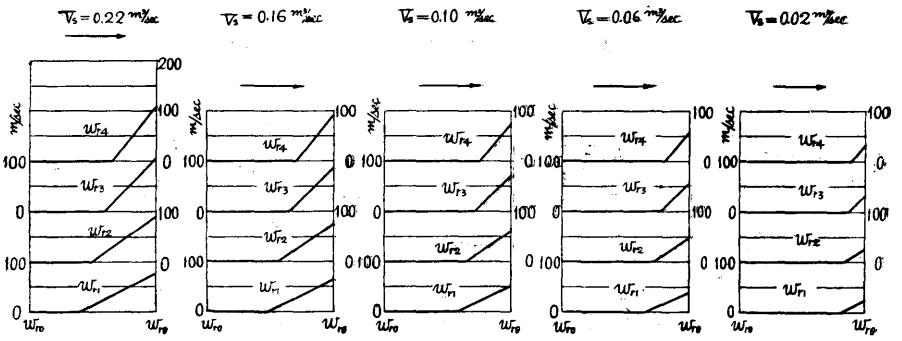

Fig. 24. Relative velocity distributions [$z=8$, $n=15000$ r.p.m.].

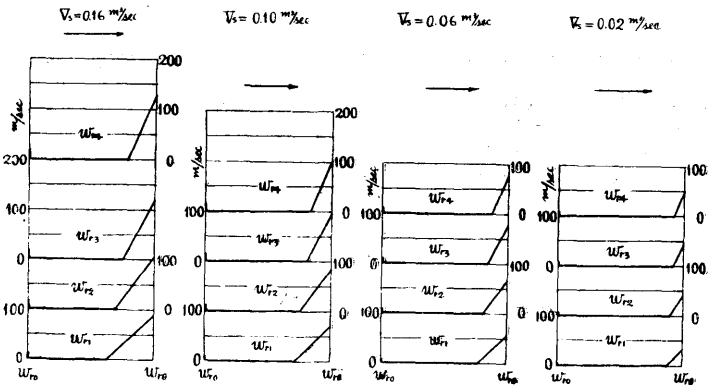

Fig. 25. Relative velocity distributions [$z=4$, $n=15000$ r.p.m.].

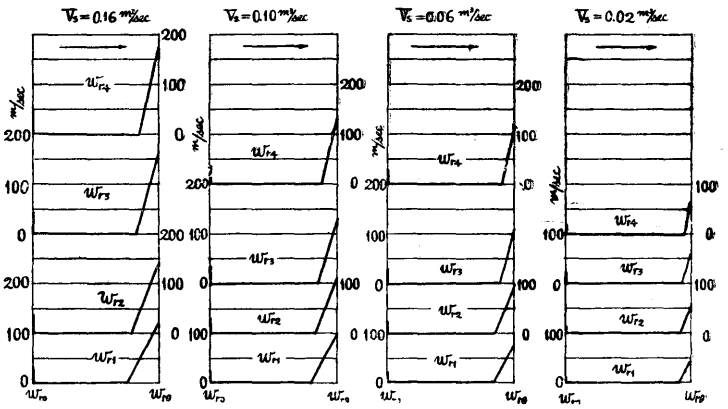

Fig. 26. Relative velocity distributions [$z=2$, $n=15000$ r.p.m.].

impeller rotations $n=15000$ r.p.m. are tabulated in table 1.

Table 1.

No. of blades	2	4	8	16	20	32
$V_{s,p_d=0}$ m³/sec	0.2875	0.3165	0.343	0.347	0.346	0.344

As is seen from the above table, it is clear that the values of $V_{s,\,p_d=0}$ takes nearly the same value except when z is 2 and 4. Taking, therefore, $V_{s,\,p_d=0}=0.345$ m³/sec as standard value, and dividing $V_s=0.22$, 0.16, 0.10, 0.06 and 0.02 m³/sec which are the parameters for the calculus of relative velocity distribution by this value, and expressing this ratio by $\lambda=V_s/V_{s,\,p_d=0}$, we obtain $\lambda=0.638$, 0.464, 0.290 0.174 and 0.058 respectively. With these values as parameters, and using the results of fig. 21~fig. 26, we can calculate the ratio of the region where the relative velocities are positive to the whole region of the impeller channel, that is the ratio of $a'/a=(\theta-\theta_0)/\theta$. These values are plotted against the number of blades z as shown in fig. 27. The values of $a'/a=(\theta-\theta_0)/\theta$ obtained from the photographic study of the relative flow in impeller channel when $n=9100$ r.p.m. are shown with small circles in the same diagram, the $G_{p_d=0}$ i.e. the mass flow of air when $\Delta p_d=0$ in this case being 0.0114 kg/sec. The figures shown besides this small circle indicate the values of λ. The estimated values of λ from the photographic study are by no means so accurate, bebause the flow patterns itself are somewhat different in every channel of the impeller. Nevertheless, the results obtained give coincidence to some extent with the results obtained numerically from the enumeration of relative velocity distribution, to find the method of calculation of relative velocity distribution abovementioned to be reliable to some degree.

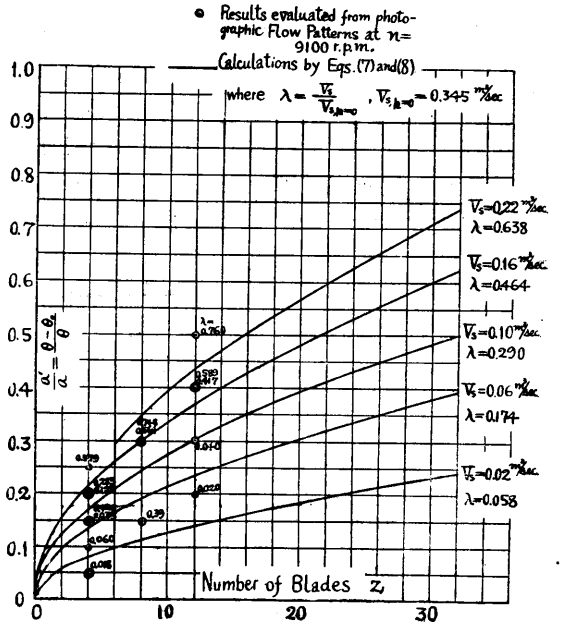

Fig. 27. Relations between $a'/a=(\theta-\theta_0)/\theta$ and number of blades [$n=15000$ r.p.m.].

We are acquainted now that the graphical method of calculation for the slip coefficient are applicable provided the proper assumptions based on the photographic study were introduced, but the evaluation are too tedious to be applied practically. Hence the author intended to establish a formula for the relation of the slip coefficient and the number of blades for the straight radial blades impeller, of which we shall treat later.

4.2 Formula for the slip coefficient of the straight radial blades impeller.

The velocity diagram at the impeller exit of a straight radial blades impeller when the number of blades are infinite is shown in full lines in fig. 28 (a), where the

peripheral component of the absolute velocity w_2 is denoted by c_{2u} which is equal to u_2. When partial flow here considered occurs, the velative velocities in the impeller channel w_{r_2}' become larger than w_{r_2}, so that the exit velocity diagram in this case become that shown by ditted lines in fig. 28 (a) taking into consideration of the slip phenomena, and the peripheral velocity component of absolute velocity w_2' become c_{2u}', to find the slip by an amount of Δc_u. The slip coefficient K in this case is given, therefore,

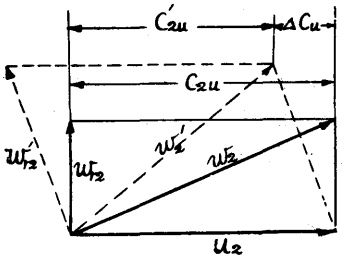

Fig. 28 (a).

$$K=\frac{c_{2u}'}{c_{2u}}=\frac{c_{2u}-\Delta c_u}{c_{2u}} \qquad \cdots(15)$$

so that we are to calculate Δc_u. To attain this end, the author followed the stodola's idea. When the partial flow is not taken into consideration, the mean relative velocity w_{r_2} at the impeller exit is [fig. 28 (b)] equal to the relative velocity when the number of blades are infinite because of the linear distribution of the relative velocity. To find the deviation of the relative velocities when th number of blades are finite, it can be considered that the relative velocity distribution when the number of blades are finite is equivalent to the rotation of the relative velocity distribution diagrams when the number of blades are infinite. To find the mean rotation, therefore, it is convenient that the square, length of the sides of which being a [fig. 28 (a)] suffers the deformation such that the sides AB and CD rotates with an angular velocity $\omega'=\Delta w/a$ because of the enlargement of the relative velocity to $w_{r_2,\theta}$, while the sides AD and BC receives no rotation. Hence, the average rotation in this case is shown in the diagram as the rotation angle of the diagonal of the square. This is Stodola's idea, and B. Eck had established the formula later shown following this idea. This mean rotation $\omega'/2$ causes the peripheral velocity component $(a/2)(\omega'/2)=\Delta w/4$ in the middle of the impeller channel, which reacts in opposite direction to c_{2u} so that the relation $\Delta c_u=\Delta w/4$ is obtained finally.

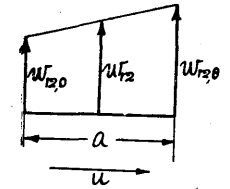

Fig. 28 (b).

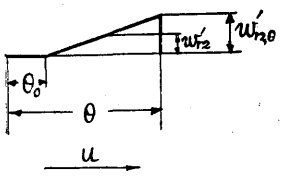

Fig. 28 (c).

If we apply this idea to the case of partial flow [fig. 28 (c)], we obtain

$$\omega'\frac{\Delta w}{\theta-\theta_0}=\frac{w'_{r_2,\theta}}{\theta-\theta_0}$$

Putting

$$\frac{1+\dfrac{r_2-r_0}{2b_2}\tan\alpha}{1+\dfrac{r_2-r_0}{b_2}\tan\alpha}=k$$

and substituting in equation (7), we get the relation

$$w_{r_2}',_{\theta}=\frac{2\omega r_2}{k}\frac{1}{2-K}(\theta-\theta_0)$$

or

$$\omega'=\frac{2\omega r_2}{k}\frac{1}{2-K}$$

and finally we obtain the expression for Δc_u as

$$\Delta c_u=\frac{\theta-\theta_0}{2}\frac{\omega'}{2}=\frac{\theta-\theta_0}{4}\omega'=\frac{\omega r_2}{2k}\frac{\theta-\theta_0}{2-K}$$

Hence,

$$K=\frac{c_{2u}'}{c_{2u}}=\frac{c_{2u}-\Delta c_u}{c_{2u}}=1-\frac{1}{2k}\frac{\theta-\theta_0}{2-K} \qquad \cdots(16)$$

By the expression obtained from equation (8)

$$\frac{V}{zb_2r_2}=\frac{\omega r_2}{k}\frac{1}{2-K}(\theta-\theta_0)^2$$

we know that

$$\theta-\theta_0=\sqrt{\frac{V_2(2-K)k}{zb_2r_2^2\omega}} \qquad \cdots(17)$$

Substituting (17) in (16) we find finally

$$K=1-\frac{1}{2}\sqrt{\frac{V_2}{(2-K)zb_2r_2^2k\omega}} \qquad \cdots(18)$$

This equation is the third order as to the slip coefficient K, and although this is able to be solved, it is too tedious to practical use as a formula. Also, it can be reduced into quadratic form, by expanding $1/(2-K)$ in the second term of the right hand side into series, and neglecting the terms of the third order of K, but, this also gives too complex expression. Hence, putting approximately $K=1$ in $1/(2-K)$ within the square root, as the effect is considered less by the square root, and we obtain

$$K=1-\frac{1}{2}\sqrt{\frac{V_2}{zb_2r_2^2k\omega}}\ ^{24)} \qquad \cdots(19)$$

where

$$k=\frac{1+\frac{r_2-r_0}{2b_2}\tan\alpha}{1+\frac{r_2-r_0}{b_2}\tan\alpha}$$

the α in the above expression being the apex angle of the sides of blade.

Stodola gives as the slip coefficient of impeller as follows.

$$K=1-\frac{u_2\pi\sin\beta_2}{z\left(u_2-\frac{V}{\pi d_2b_2\tan\beta_2}\right)} \qquad \cdots(20)$$

where β_2: exit angle of the blade.

24) V_2 is the volume flow at the impeller exit, and when V_2 is unknown we can use the value of V_s instead of V_2 with negligible error.

B. Eck gives, in his text book, the following formula, thus

$$K=\frac{1}{1+\dfrac{\sin\beta_2\pi d_2^2 b_2}{8Sz}} \qquad \cdots(21)$$

where S is the side surface area of the blade, and when the shape of the blade is of trapezoid whose inner breadth is b_1 (at radius r_1) and outer breadth is b_2 (at radius r_2) it is expressed as

$$S=\left(r_2-\frac{r_2-r_1}{3}\frac{2b_1+b_2}{b_1+b_2}\right)\frac{b_1+b_2}{2}(r_2-r_1)$$

Pfleiderer's formula is of the form:

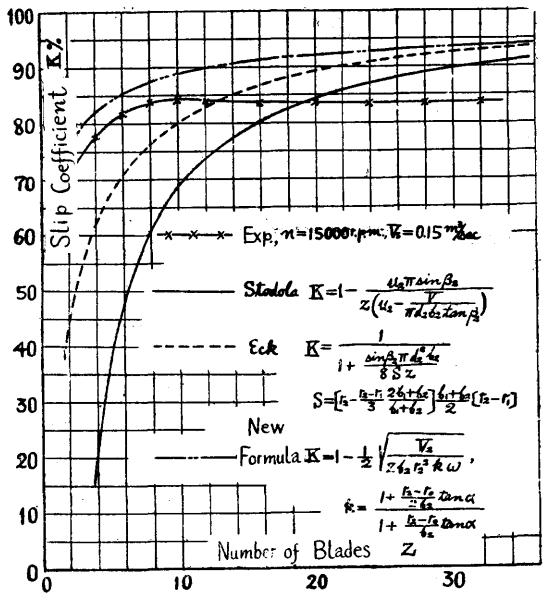

Fig. 29. Comparison of new formula with experimental results.

$$K=\frac{1}{1+\dfrac{\Psi}{z}\dfrac{r_2^2}{S}} \qquad \cdots(22)$$

but in this case Ψ is the experimental value, aud as the values of Ψ for the radial exit impeller are not shown, this formula is not used in the present case.

The comparisons of the experimental data when n=15000 r.p.m. and V_s=0.15 m³/sec to the results of evaluations by the new formula of (19), Stodola's formula (20) and Eck's formula of (21) are shown in fig. 29. As previously stated, the relation between the slip coefficient of impeller and the number of blades for the high speed straight radial blades impeller is quite dif-

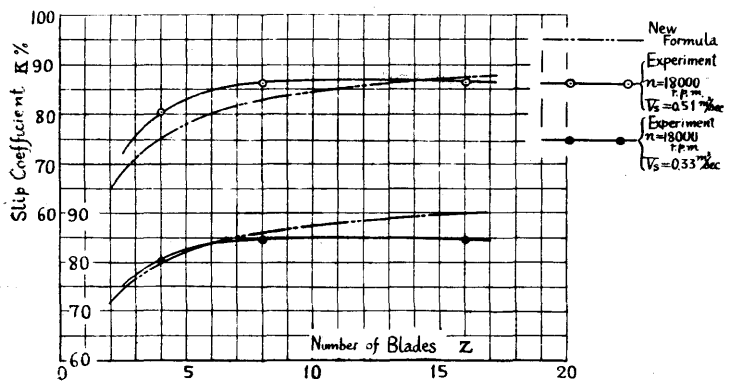

Fig. 30.
Comparison of new formula with another experimental results.

ferent that for the backward curved blades impeller, and as is clear in fig. 29, Stodola's formula or Eck's formula shows coincidence no longer, while the new formula (19) coincides approximately with experimental results. The comparison of the results of another blower of straight radial blades, the number of which being 4, 8 and 16, with the caluclated value by (19) is shown in fig. 30, which shsws less deviations than in fig. 29. Therefore, the new formula is applicable for the straight radial blades impeller to some extent.

V. Conclusioni.

The conclusions obtained by these experiments and considerations can be abstracted as follows.

(1) The performance characteristics of a entrifugal blower show optimum at certain number of blades. When the number blades is less than this optimum value, the performances become inferior on account of partial flow within the impeller channel, wrile when the number of blades exceeds the optimum value, the performances also show lower value on account of the increase of flow resistances in impeller channel. Although the optimum number of blades of the centrifugal blower with straight radial blades is found to be $z=10\sim12$ in this case, this figure is not applicable in general, even if the shape of blades be the same. The optimum number of blades seems to be affected intensively by the diameter ratio of the impeller, and the larger the diameter ratio, i.e. the longer the blades, the less the optimum number of blades, from the experiments by the author himself and from the references already cited to. But it is unable to formulate this effect completely on account of shortness of experimental data.

(2) The ration of the ship coefficient of impeller to the number of blades for the straight radial blades impeller is quite different to the generally used impeller of backward curved blades type. The results of graphical calculation coincide with experimental results, by means of the correction of the hitherto used Eck's method by the assumptions obtained from the photographic study of the flow patterns within the impeller channel. Stodola's formula or Eck's formula is no longer applicable to the cases of high speed straight radial blades imdeller as treated in this paper, while the now formula obtained shows some coincidence with experimental results.

On Two Kinds of Fluid-Flow through Bent-Pipes.

Recieved Jan. 15, 1949.

Fumiki Kito*

Two kinds of Vortex motions occurring in bent-pipe has been studied theoretically. The first is the secondary vortex flow produced in a bent pipe of elliptical cross-section; the flow being supposed to be in the state of so-called laminar flow. The second case concerns

* Dr. of Eng. Prof. of Keiogijuku University.